



HAL
open science

Setting a chronology for the basal ice at Dye-3 and GRIP: Implications for the long-term stability of the Greenland Ice Sheet

Audrey M. Yau, Michael I. Bender, Thomas Blunier, Jean Jouzel

► **To cite this version:**

Audrey M. Yau, Michael I. Bender, Thomas Blunier, Jean Jouzel. Setting a chronology for the basal ice at Dye-3 and GRIP: Implications for the long-term stability of the Greenland Ice Sheet. *Earth and Planetary Science Letters*, 2016, 451, pp.1-9. 10.1016/j.epsl.2016.06.053 . hal-03108179

HAL Id: hal-03108179

<https://hal.science/hal-03108179>

Submitted on 24 Jun 2021

HAL is a multi-disciplinary open access archive for the deposit and dissemination of scientific research documents, whether they are published or not. The documents may come from teaching and research institutions in France or abroad, or from public or private research centers.

L'archive ouverte pluridisciplinaire **HAL**, est destinée au dépôt et à la diffusion de documents scientifiques de niveau recherche, publiés ou non, émanant des établissements d'enseignement et de recherche français ou étrangers, des laboratoires publics ou privés.

1
2
3
4
5
6
7
8
9
10
11
12
13
14
15
16
17
18
19
20
21

Setting a Chronology for the Basal Ice at Dye-3 and GRIP: Implications for the Long-Term Stability of the Greenland Ice Sheet

Audrey M. Yau^a, Michael L. Bender^{a,b,*}, Thomas Blunier^c, Jean Jouzel^d

^a*Department of Geosciences, Princeton University, Princeton NJ, 08540 USA*

^c*Institute of Oceanology, Shanghai Jiao Tong University, 800 Dongchuan Rd., Minhang, Shanghai, China. 200240*

^b*Centre for Ice and Climate, Niels Bohr Institute, University of Copenhagen, Juliane Maries Vej 30, DK-2100 Copenhagen, Denmark*

^d*Laboratoire des Sciences du Climat et de l'Environnement, CEA-CNRS-University Versailles-Saint Quentin, CE Saclay, Orme des Merisiers, 91191 Gif-sur-Yvette, France*

*Corresponding author: bender@princeton.edu, (609) 258-2936.

Key Words: Greenland Ice Sheet; Dye-3; GRIP; Ar-dating; ¹⁷Δ stratigraphy

22 **Abstract**

23 The long-term stability of the Greenland Ice Sheet (GIS) is an important issue in our
24 understanding of the climate system. Limited data suggest that the northern and southern sections
25 extend well back into the Pleistocene, but most age constraints do not definitively date the ice.
26 Here, we re-examine the GRIP and Dye-3 ice cores to provide direct ice core observations as to
27 whether the GIS survived previous interglacials known to be warmer (~130 ka) or longer (~430
28 ka) than that of the present interglacial. We present geochemical analyses of the basal ice from
29 Dye-3 (1991-2035 m) and GRIP (3020-3026 m) that characterize and date the ice. We analyzed
30 the elemental and isotopic composition of O₂, N₂, and Ar, of trapped air in these two cores to
31 assess the origin of trapped gases in silty ice. Dating of the trapped air was then achieved by
32 measuring the paleoatmospheric $\delta^{40}\text{Ar}/^{38}\text{Ar}$ and the ¹⁷O anomaly (¹⁷Δ) of O₂. The resulting age is
33 a lower limit because the trapped air maybe contaminated with crustal radiogenic ⁴⁰Ar. The
34 oldest average age of replicates measured at various depths is 970 ± 140 ka for the GRIP ice core
35 and 400 ka ± 170 ka for Dye-3. ¹⁷Δ data from Dye-3 also argue strongly that basal ice in this core
36 predates the Eemian. This confirms that the Greenland Ice Sheet did not completely melt at
37 Southern Greenland during the last interglacial, nor did it completely melt at Summit Greenland
38 during the unusually long interglacial ~ 430 kyr before present.

39

40 **Key Words:** Greenland Ice Sheet; Dye-3; GRIP; Ar-dating; ¹⁷Δ stratigraphy

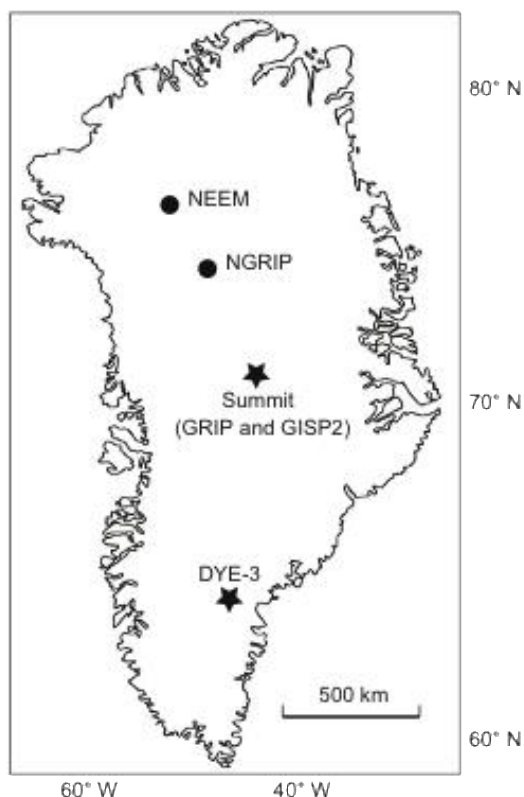
41

42 **1. Introduction**

43 The Greenland Ice Sheet is the second largest reservoir of water on land, and if
44 completely melted, would contribute roughly 7 m to global eustatic sea level (Bamber et al.,
45 2013). As a large, climate sensitive source to sea level rise, the response of the Greenland Ice
46 Sheet (GIS) to global warming has been an important, debated subject. Understanding the
47 response of the GIS to past climate change events, such as previous interglacials, can provide a
48 more accurate context for how anthropogenic global warming may impact the GIS in the future.
49 Here, we advance the understanding of the long-term stability of the ice sheet by dating trapped
50 air from the base of two Greenland ice cores (Fig. 1). By dating the trapped air from the deepest
51 ice of the GRIP ice core, located at Summit Greenland, and the Dye-3 ice core, located in
52 Southern Greenland, we determine, from direct observations, the minimum age after which an
53 ice sheet existed at these sites. In establishing this age, we determine whether the GIS has
54 persisted through interglacials such as the Eemian, when Arctic temperatures were 3-5°C warmer
55 than today and sea level was 6-9 m higher than today (Clark and Huybers, 2009; Kopp et al.,
56 2009) or Marine Isotope Stage 11 (400-430 ka), which was much longer than the present
57 interglacial.

58 Previous studies on the trapped air in ice cores have established the antiquity of an ice
59 sheet at Summit (GRIP and GISP2) and Northern Greenland (NEEM) through at least the last
60 interglacial (115-130 ka), and probably back to Marine Isotope Stage 7, ~235 ka (Chappellaz et
61 al., 1997; Suwa et al., 2006; Dahl-Jensen, 2013; Yau, PhD Thesis). However, an ongoing
62 discussion persists on the minimum age of the deepest ice at Summit Greenland (GRIP) and
63 Southern Greenland (Dye-3) because basal ice at these sites is stratigraphically disturbed
64 (Johnsen et al., 2001; Verbeke et al., 2002; Tison et al., 1994; Bender et al., 2010). Of particular

65 interest is the question of whether the GIS survived at these sites through Marine Isotope Stage
66 (MIS) 11, an unusually long interglacial when mean global sea level may have been 6-13 m
67 above present (Raymo and Mitrovica, 2012).



68
69 Fig. 1. Greenland ice core sites with possible Eemian-aged basal ice. Ice cores discussed in this
70 study are starred.

71
72 Ice at the base of the glacier has properties that originate in several different ways. “Dry
73 densified ice” forms via the accumulation and burial of dry snow (Herron and Langway, 1980).
74 “Wet origin ice” was partly or completely melted at some point in its history. Wet origin ice
75 would include frozen soils, lake water, partly melted basal ice, and superimposed ice.

76 Dry densified ice has a total gas content of ~ 100 scc/kg (standard cubic centimeters of
77 gas/kg of ice). The exact value depends on elevation (higher at low elevation), temperature

78 (higher at colder temperatures), and summer insolation. Wet origin ice has a much lower gas
79 content (except for metabolic CO₂ and CH₄), because the solubility of gas in water is much less
80 than 100 scc/kg, and because gases may be exsolved upon freezing. If one mixes comparable
81 amounts of dry densified and wet origin ice, the dry component will dominate the gas mixture.
82 “Silty ice” sampled at the base of deep ice cores is generally dry origin ice mixed with some
83 amount of either locally formed ice from the initial growth stages of the ice sheet (Tison et al.,
84 1994; Souchez et al., 1994) or another basal component such as soil, permafrost, preglacial snow,
85 lake ice, or ground ice (Bender et al., 2010). We use the term “clean ice” to describe ice free of
86 visible silicate impurities. All clean ice samples in this paper are believed to be dry densified.

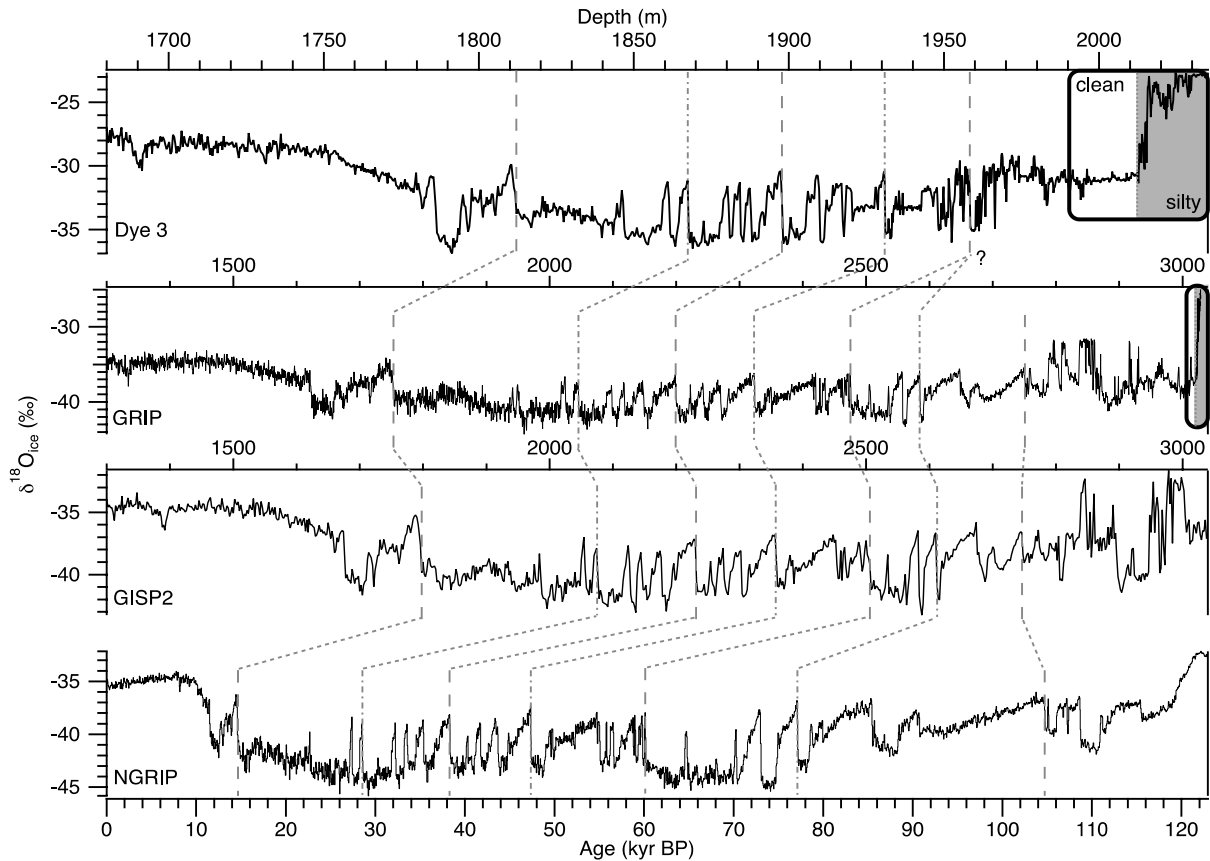
87 Previous studies have estimated that the silty basal ice, from 3022-3029 m depth in the
88 GRIP ice core, could be as old as 2.4 Ma, dating to the original build-up of the GIS (Souchez et
89 al., 1994; Souchez et al., 2006). Souchez et al. (2006) and Tison et al. (1998) found several
90 indications of biological activity that indicated a soil source for the silty particles found in the
91 bottom 7 m of GRIP. These included organic matter that was present in swampy areas, drawing
92 down the O₂ concentration to 10% of saturation, very high concentrations of methane, high
93 concentrations of NH₄⁺, and the presence of ammonium oxalate, which they attributed to the
94 breakdown of bird droppings in local soils. They deduced that central Greenland was vegetated
95 at the time the silty ice formed, and that traces of ancient soil were preserved in a snowdrift that
96 was overridden by the ice sheet. ¹⁰Be/³⁶Cl dating by Willerslev et al. (2007) gives an age of the
97 silty basal ice of 950 ± 44 ka. The uncertainty is calculated from ³⁶Cl and ¹⁰Be abundance errors
98 only, and the authors have noted several factors that could cause the ³⁶Cl/¹⁰Be age to be either
99 younger or older than the true age of the ice. Here, we revisit the basal ice of the GRIP ice core

100 to confirm the antiquity of the trapped air of this ice inferred by Souchez et al. (1994, 2006) and
101 Willerslev et al. (2007).

102 Willerslev et al. (2007) also concluded that basal ice from Southern Greenland at Dye-3
103 is likely 450-800 ka. They presented results from a number of dating techniques (amino acid
104 racemization, $^{10}\text{Be}/^{36}\text{Cl}$, and optical stimulated luminescence dating), each with its own set of
105 assumptions and uncertainties, which collectively suggest that the Dye-3 silty ice dates to this
106 age. However, the assumptions and uncertainties were large enough that Willerslev et al. (2007)
107 were unable to conclusively rule out the possibility that the basal silty ice of Dye-3 may date
108 only to the last interglacial (115-130 ka). Independent support for a pre-Eemian age for the
109 southern GIS comes from sediment flux data from the southern Greenland margin (Colville et al.,
110 2011; Reyes et al., 2014). While these studies have pointed to the antiquity and stability of the
111 southern GIS through Arctic warm periods, earlier studies on the Dye-3 ice core inferred that the
112 southern GIS did not persist through the Eemian. Koerner et al. (2002) argued that this region
113 was ice-free during the last interglacial, as no isotopically cold ice exists below the warm basal
114 section (Fig. 2). Other research highlights the abrupt and large increase with depth in $\delta^{18}\text{O}_{\text{ice}}$
115 ($\sim 8\text{‰}$) over a very short interval (2012-2016 m). Koerner (1989) and Souchez et al., (1998)
116 suggest that the silty basal ice is a completely separate unit of ice that was accreted onto the
117 bottom of the overlying dry origin clean ice that makes up the bulk of the glacier at Dye 3 and
118 GRIP, respectively (Fig. 2).

119 We analyzed samples from the clean and silty units of the Dye-3 ice core between 1991-
120 2035 m and the GRIP ice core between 3020-3026 m. At Dye 3, $\delta^{18}\text{O}$ of the ice is nearly
121 constant between 1990-2012 m depth at -31‰ (Holocene $\delta^{18}\text{O} = -27\text{‰}$) (Fig. 2). Silty ice first
122 appears at ~ 2012 m in the Dye-3 ice core. From there to the bottom, at 2025 m depth, $\delta^{18}\text{O}$ lies in

123 the range -24 to -26 ‰. At GRIP, silty ice first appears at 3022.25 m. From there to the bottom,
 124 $\delta^{18}\text{O}$ rises from about -36 to -25‰. By focusing on the trapped air in ice, we mainly characterize
 125 the dry densified ice component of the silty ice, rather than the wet origin component, which
 126 bears the silt, and has a lower total gas content (Boereboom et al., 2013). However, wet based ice,
 127 or other locally derived ice such as ice wedges, may still have substantial total gas contents
 128 (Boereboom et al, 2013). Therefore, gas ages may be aliased by wet-origin ice predating the
 129 growth of the ice sheet. Methods dating basal ice by measuring non-gas properties, such as U-
 130 series recoil dating, primarily access the wet-origin ice, and may very well give different ages.



131
 132 Fig. 2. Comparison of $\delta^{18}\text{O}_{\text{ice}}$ for Dye-3, GRIP, GISP2, and NGRIP ice cores. Dye-3, GRIP, and
 133 GISP2 are plotted on the top axis versus depth. NGRIP is plotted on the bottom axis versus age.
 134 Dotted lines show $\delta^{18}\text{O}_{\text{ice}}$ matching between cores. GRIP and GISP2 are chronologically

135 continuous to ~105 ka, and Dye-3 is chronologically continuous to ~60 ka. The bold boxes
136 highlight the analyzed sections of Dye-3 and GRIP. The shaded portion indicates silty basal ice.

137

138 To determine the conditions during the trapping of air, we measured the elemental and
139 isotopic composition of O₂, N₂, and Ar. We report the composition units with respect to air in the
140 standard δ notation with units in ‰ (per mil):

$$141 \quad \delta = [R/R_o - 1]$$

142 where δ is the fractional deviation of a gas pair ratio R from a reference (air) ratio R_o . These
143 analyses tell us whether the trapped air has been gravitationally or thermally fractionated ($\delta^{15}\text{N}$
144 and $\delta^{38}\text{Ar}/^{36}\text{Ar}$), partially melted ($\delta\text{Ar}/\text{N}_2$), or microbially respired ($\delta^{18}\text{O}$ of O₂, $\delta\text{O}_2/\text{N}_2$, and
145 $\delta\text{O}_2/\text{Ar}$).

146 We also date the trapped air from both cores by measuring the paleoatmospheric
147 $\delta^{40}\text{Ar}/^{38}\text{Ar}$ (Bender et al., 2008), and we present measurements of $^{17}\Delta$ of O₂ (Blunier et al., 2002;
148 Blunier et al., 2012) that help constrain the age of basal Dye-3 ice. These analyses contribute to
149 our understanding of the origin of the basal ice from Dye-3 and GRIP, and how old this ice may
150 be. These results provide useful constraints on the long-term stability of the GIS and models
151 predicting its evolution in response to global change.

152

153 **2. Methods**

154 Interpreting gas properties requires a correction for gravitational fractionation. This term
155 refers to the fact that, in a diffusive environment, heavy gases and isotopes are progressively
156 enriched with depth according to the barometric equation. The enrichment scales with mass
157 difference (Craig et al., 1988). We measure gravitational enrichment from $\delta^{15}\text{N}$ and $\delta^{38}\text{Ar}/^{36}\text{Ar}$.

158 Gases may also be biased from the atmospheric composition by thermal fractionation. The effect
159 of thermal fractionation is discussed in section 3.2.

160

161 **2.1 Age Reconstruction – Ar-chronometer**

162 We have dated the trapped air of the deepest GRIP and Dye-3 ice by the Ar-isotope
163 method (Bender et al., 2008). The chronometer makes use of the fact that ^{36}Ar and ^{38}Ar have
164 been essentially constant throughout recent geologic time, but ^{40}Ar has been slowly increasing in
165 the atmosphere as a result of the decay of ^{40}K . $\delta^{40}\text{Ar}/^{38}\text{Ar}$ has been measured in ice cores to 800
166 ka. Over this period, it has risen at a rate of $0.066 \pm 0.007\text{‰}/\text{Ma}$. We precisely measure the
167 $\delta^{40}\text{Ar}/^{38}\text{Ar}$ of the trapped air and determine the age of the air based on this rate of $\delta^{40}\text{Ar}/^{38}\text{Ar}$
168 increase.

169 The analytical method is similar to that described by Bender et al. (2008). Trapped air
170 was extracted using a wet-melting technique, where ice was melted in an evacuated glass flask.
171 The sample was then equilibrated with meltwater, and the meltwater was removed as outlined by
172 Emerson et al. (1995). The sample gas was then passed through a water trap submerged in liquid
173 N_2 , in which residual water and CO_2 were frozen out. Ar was purified from the remaining gases
174 through exposure to a getter which, when activated, reacts with and removes non-noble gases.
175 The remaining gas was captured in a stainless steel tube submerged in liquid helium. After
176 warming to room temperature, the sample was then analyzed on a Finnigan MAT 252 mass
177 spectrometer with collectors specific to ^{36}Ar , ^{38}Ar , and ^{40}Ar .

178 Samples and air standards (modern air collected from the roof of the Princeton University
179 Geosciences building in New Jersey) were run in three different analytical periods. The standard
180 deviations of samples run in period 1 (n=7) for $\delta^{40}\text{Ar}/^{38}\text{Ar}$, $\delta^{38}\text{Ar}/^{36}\text{Ar}$, and $\delta^{40}\text{Ar}/^{36}\text{Ar}$ were

181 $\pm 0.018\%$, $\pm 0.052\%$, and $\pm 0.035\%$ respectively. For period 2 (n=23), standard deviations were
182 $\pm 0.016\%$, $\pm 0.034\%$, and $\pm 0.020\%$. For period 3 (n=7), standard deviations were $\pm 0.008\%$,
183 $\pm 0.023\%$, and $\pm 0.019\%$. Table 1 indicates in which suite each sample was analyzed.

184

Table 1. Dating by Ar- and O₂-isotope composition w.r.t. air. Each line represents a single analysis.

GRIP ice core						
Depth (m)	Analysis Period ^o	$\delta^{40}\text{Ar}/^{38}\text{Ar}$ (‰)	$\delta^{40}\text{Ar}/^{36}\text{Ar}$ (‰)	$\delta^{38}\text{Ar}/^{36}\text{Ar}$ (‰)	$\delta^{40}\text{Ar}/^{38}\text{Ar}_{\text{atm}}$ (‰)	Age (ka)
3020	3	0.746	1.540	0.793	-0.048	710
3020	3	0.762	1.550	0.788	-0.027	390
3022	3	0.675	1.43	0.757	-0.083	1240
3022	3	0.713	1.482	0.77	-0.058	860
3025	3	0.454	0.963	0.509	-0.056	830
3025	-	-	-	-	-	-
3026	3	0.44	0.88	0.44	0	-10
3026	3	0.428	0.896	0.467	-0.039	580

*Shaded section denotes samples from the silty basal ice

^oSee Methods

Analytical uncertainty for a single sample is ± 250 ka

Dye-3 ice core							
Depth (m)	Analysis Period ^o	$\delta^{40}\text{Ar}/^{38}\text{Ar}$ (‰)	$\delta^{40}\text{Ar}/^{36}\text{Ar}$ (‰)	$\delta^{38}\text{Ar}/^{36}\text{Ar}$ (‰)	$\delta^{40}\text{Ar}/^{38}\text{Ar}_{\text{atm}}$ (‰)	Age (ka)	¹⁷ Δ of O ₂ (per meg)
2004	-	-	-	-	-	-	40.4
2004	-	-	-	-	-	-	29.6
2008	-	-	-	-	-	-	49.1
2008	-	-	-	-	-	-	47.2
2011	1	0.569	1.155	0.586	-0.017	260	-
2011	2	0.617	1.268	0.650	-0.035	530	-
2015	2	0.223	0.436	0.213	0.010	-150	-
2015	-	-	-	-	-	-	-
2019	1	0.238	0.462	0.224	0.014	-210	-
2019	2	0.150	0.285	0.135	0.015	-230	-
2023	-	-	-	-	-	-	36.1
2023	-	-	-	-	-	-	42.6
2031	2	0.196	0.382	0.186	0.010	-150	53.6
2031	-	-	-	-	-	-	48.0
2035	2	0.246	0.473	0.227	0.019	-280	-
2035	-	-	-	-	-	-	-

*Shaded section denotes samples from the silty basal ice

^oSee Methods

Analytical uncertainty for a single sample is ± 250 ka

186 The term of merit for dating, $\delta^{40}\text{Ar}/^{38}\text{Ar}_{\text{atm}}$ (paleoatmospheric $\delta^{40}\text{Ar}/^{38}\text{Ar}$), is defined as

187
$$\delta^{40}\text{Ar}/^{38}\text{Ar}_{\text{atm}} = \delta^{40}\text{Ar}/^{38}\text{Ar} - 1.002 * \delta^{38}\text{Ar}/^{36}\text{Ar} \quad (1)$$

188 The second term corrects for gravitational fractionation. The standard deviation of $\delta^{40}\text{Ar}/^{38}\text{Ar}_{\text{atm}}$
189 values, normalized to the means of their analysis periods, is $\pm 0.016\text{‰}$ ($n = 37$). The
190 corresponding age uncertainty is ± 250 kyr (1σ) for a single sample. During the first two analysis
191 periods, 12 Holocene-aged ice samples (Newall Glacier ice core) were also analyzed using the
192 same extraction technique applied to samples (one Newall sample was removed as an outlier)
193 yielding an average age of 130 ± 150 ka (1σ). During the third analysis period, 3 samples
194 inferred to have Holocene air (shallow ice from Mullins Valley, Antarctica with modern air due
195 to cracks in the surface ice, $< 5\text{m}$ depth) were analyzed, yielding an average age of 110 ± 230 ka
196 (1σ).

197

198 **2.2 Age Reconstruction – $^{17}\Delta$ of O_2 Stratigraphy**

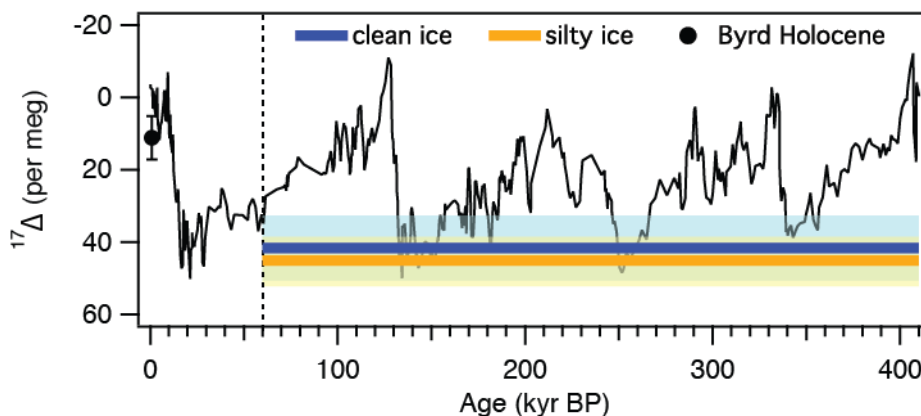
199 A second technique was used to constrain the age of the basal ice at Dye-3, which
200 involved analyzing the $^{17}\Delta$ of O_2 (the triple isotopic composition of O_2), defined as:

201
$$^{17}\Delta = (\ln(\delta^{17}\text{O}_{\text{atm}} + 1) - 0.516 * \ln(\delta^{18}\text{O}_{\text{atm}} + 1))$$

202
$$\approx \delta^{17}\text{O}_{\text{atm}} - 0.516 * \delta^{18}\text{O}_{\text{atm}} \quad (2)$$

203 The coefficient (0.516) is the fractionation ratio for $^{17}\text{O}/^{16}\text{O}$ of O_2 relative to $^{18}\text{O}/^{16}\text{O}$ (Luz et al.,
204 1999). This technique exploits the fact that $^{17}\Delta$ is a measure of the non mass-dependent
205 fractionation of O_2 , which originates in O_2 - CO_2 exchange in the stratosphere (Luz et al., 1999).
206 $^{17}\Delta$ changes with time in the atmosphere, and the record is known for the past 400 ka from the
207 Vostok, Siple, and GISP2 ice cores (Fig. 3; Blunier et al., 2012). To a first approximation, $^{17}\Delta$

208 tracks contemporaneous CO₂ (Blunier et al., 2012). ¹⁷Δ data are given in per meg where 1 per
209 meg corresponds to 0.001 ‰.



210
211 Fig. 3. Mean of ¹⁷Δ of O₂ for Dye-3 clean and silty ice plotted versus age. In black, a 3-point
212 smoothing of ¹⁷Δ of O₂ for the past 400 ka from Vostok, GISP2, and Siple (Blunier et al., 2012).
213 In yellow, ¹⁷Δ of O₂ for silty ice; mean = 45 ± 7 per meg (1σ in light yellow; st. error = ±4 per
214 meg). In blue, ¹⁷Δ of O₂ for clean ice; mean = 42 ± 9 per meg (1σ in light blue; st. error = ±4 per
215 meg). The black circle is the average of Byrd Holocene samples; mean 11 ± 6 per meg (1σ). The
216 dashed line marks 60 ka, the minimum age for the deep ice (see Fig. 2). Mean values for both the
217 clean and silty ice are comparable to glacial maximum values observed for deep ice cores,
218 indicating the air is at least as old as 132 ka.

219
220 Given the definition of ¹⁷Δ, microbial respiration of air (a mass-dependent fractionation
221 process) does not contaminate this record, as it causes δ¹⁷O_{atm} to change at a rate equal to 0.516
222 times the change in δ¹⁸O_{atm}. In contrast, metabolic production or consumption of gases in silty
223 ice alters all other properties used for gas stratigraphy in ice cores, including CO₂, CH₄, and
224 δ¹⁸O_{atm} (paleoatmospheric δ¹⁸O of O₂). This is an important distinction as the basal silty ice of
225 Dye-3 is contaminated by microbial respiration, with CO₂ values observed up to 36,000 ppmv

226 (Souchez et al., 1998); consequently, these gas properties cannot be used for chemostratigraphy.
227 Here, we make use of the fact that saw-tooth, 100-kyr glacial-interglacial CO₂ cycles are
228 observed in the ¹⁷Δ record (Blunier et al., 2002; Blunier et al., 2012), which can be used to place
229 samples in the context of the global climate state.

230 The triple isotope composition of oxygen (¹⁷Δ) was determined by processing air
231 extracted from ~50 g of ice through a vacuum line connected to a gas chromatograph as per
232 Blunier et al. (2002). ¹⁷Δ is calculated by using δ¹⁵N to gravitationally correct both δ¹⁷O and
233 δ¹⁸O, which are then used in eqn. (2). The analytical uncertainty in ¹⁷Δ, based on the analysis of
234 modern air standards, is ±6 per meg (1σ, n = 6). 5 Holocene-aged ice samples (Byrd ice core
235 ~200-500m depth) were also analyzed using the same sampling technique applied to ice core
236 samples, yielding a Holocene ¹⁷Δ of 11 ± 6 per meg (1σ). All ¹⁷Δ values are normalized to that of
237 modern air.

238

239 **2.3 Analyses of the Elemental and Isotopic Composition of O₂, N₂, and Ar**

240 Measurements of the elemental and isotopic composition of air (δ¹⁵N, δ¹⁸O of O₂, δAr/N₂,
241 δO₂/N₂, and δO₂/Ar) were performed using the same wet-melting extraction technique applied
242 for the Ar-dating. In these extractions, ~20g of ice were used, and samples were passed through a
243 water trap in liquid nitrogen and directly captured in a 12 scc stainless steel tube submerged in
244 liquid helium. The sample was then warmed to room temperature and analyzed on a Finnigan
245 Delta Plus XP mass spectrometer. The standard deviation of modern air standards (n = 8),
246 processed as samples, were: δ¹⁵N = ±0.016‰; δ¹⁸O of O₂ = ±0.023‰; δAr/N₂ = ±0.24‰;
247 δO₂/N₂ = ±0.45‰; δO₂/Ar = ±0.34‰. The paleoatmospheric δ¹⁸O of O₂, δ¹⁸O_{atm}, is equal to

248 $\delta^{18}\text{O}$ corrected for gravitational fractionation: $\delta^{18}\text{O}_{\text{atm}} = \delta^{18}\text{O} - 2.01 * \delta^{15}\text{N}$. The standard
249 deviation is $\pm 0.024\text{‰}$.

250

251 **3. Results and Discussion**

252 **3.1 Characteristics of dry densified ice**

253 Typical dry densified ice has about 100 scc of air per kg (Herron and Langway, 1987).

254 Holocene ice at Summit has a total gas content of ~ 90 scc/kg, and the total gas content of
255 Holocene Dye-3 ice is likely higher (Martinerie et al., 1992).

256 Dry densified ice is also characterized by near-zero values of $\delta\text{Ar}/\text{N}_2$, $\delta\text{O}_2/\text{N}_2$, and $\delta\text{O}_2/\text{Ar}$
257 taking ambient air as the reference (Sowers et al., 1989; Bender et al., 1995). Values for $\delta\text{Ar}/\text{N}_2$
258 typically range between -10‰ and 0‰ in dry densified ice. These ratios are slightly depleted due
259 to the preferential loss of Ar relative to N_2 during bubble close-off, because Ar atoms are smaller
260 than N_2 molecules (Craig et al., 1988). $\delta\text{Ar}/\text{N}_2$ values above 0‰ are indicative of partially
261 melted and refrozen ice, as the solubility ratio of Ar/N_2 is approximately 2/1. $\delta\text{O}_2/\text{N}_2$ and $\delta\text{O}_2/\text{Ar}$
262 values of dry densified ice are generally slightly lower than the ratios in air, and are between -
263 25‰ to 0‰ (Sowers et al., 1989; Bender et al., 1995). Depletions below these ratios indicate
264 microbial respiration, which results in the consumption of O_2 (Souchez, 1997). Microbial
265 respiration also results in the enrichment of $\delta^{18}\text{O}_{\text{atm}}$ (modern air = 0‰ ; paleo-atmospheric range
266 = -0.4 to $+1.4$ (Dreyfus et al., 2007)), as microbes preferentially consume ^{16}O relative to ^{18}O .

267 In the firn densification process, air is fractionated by gravity, which results in the
268 enrichment of heavier isotopes with depth (Craig et al., 1988; Schwander, 1989). Gravitational
269 fractionation occurs in the firn layer and is preserved in ice once the close-off density is reached.
270 ^{15}N is enriched in the trapped air of dry origin ice, with $\delta^{15}\text{N}$ typically between 0.2 - 0.5‰

271 (modern air = 0‰), corresponding to a close-off depth of ~40-100 m. This means that for every
272 20 m depth increase in the firn, $\delta^{15}\text{N}$ is enriched by ~0.1‰. If the basal ice of GRIP and Dye-3 is
273 formed by the dry compaction of snow in a climate similar to that of today and at the top of the
274 central ice sheet, we would expect to find the following characteristics: total gas content ~100
275 scc/kg; $\delta^{15}\text{N}$ from ~-0.2-0.5‰; values of $\delta^{18}\text{O}_{\text{atm}}$ within the paleo-atmospheric range (about -
276 0.4‰ to +1.5‰); and Ar/N₂ values slightly below that of modern air.

277 The presence of liquid water will force elemental ratios of $\delta\text{Ar}/\text{N}_2$, $\delta\text{O}_2/\text{N}_2$, and $\delta\text{O}_2/\text{Ar}$
278 towards water saturation ratios rather than atmospheric ratios in wet origin ice (Fig. 4). A buried
279 perennial snowbank may have elemental ratios close to that of air, and its trapped air would be
280 gravitationally fractionated. However, the magnitude would be small because of the limited
281 depth, and might be attenuated by convection (Severinghaus et al., 2010). Snowbank air could be
282 thermally fractionated as well. (In thermal fractionation, temperature gradients associated with
283 seasonal temperature fluctuations can fractionate atmospheric ratios and isotopes both negatively
284 and positively; Chapman and Cowling, 1970; Severinghaus et al., 2001.) Low total air contents,
285 elemental ratios drawn towards water saturation ratios, and variable isotopic signatures
286 (reflecting contributions of different processes) would be expected in wet origin basal ice.

287

288 **3.2 Characteristics of GRIP and Dye-3 Basal Ice**

289 Table 2 and Figs. 4 and 5 summarize the geochemical data for the trapped air of the deep
290 GRIP and Dye-3 ice. $\delta\text{Ar}/\text{N}_2$ is plotted vs. $\delta\text{O}_2/\text{Ar}$ for the GRIP and Dye-3 samples, along with
291 data for various examples of wet origin ice (Fig. 4; Cardyn et al., 2007; Lacelle et al., 2011).

292 Air trapped in firn from Dye-3 and GRIP have the following characteristics. First, Ar/N₂
293 ratios are close to atmospheric (Fig. 4). Ratios are slightly elevated in silty GRIP (+37‰) and

294 Dye-3 (+26‰) ice, perhaps due to a small wet origin component (Souchez et al., 1988; Knight,
295 1997). However, they are nowhere near the saturation value ($\sim+1000\text{‰}$). Second, N_2 and Ar
296 isotopes both show normal gravitational enrichments (Fig. 5). The exceptions are in the two
297 deepest dirty GRIP samples, where $\delta^{38}\text{Ar}/^{36}\text{Ar}$ is much less than $2 \times \delta^{15}\text{N}$, and in the silty Dye-3
298 ice, where the enrichments are only $\sim 0.1\text{‰}$ per mass unit. Third, total air content values in silty
299 ice from GRIP and Dye-3 are significantly lower than the overlying clean ice (Table 3; Souchez
300 et al., 1995a; Souchez et al., 1998). And fourth, evidence for microbial respiration is clear with
301 $\delta^{18}\text{O}_{\text{atm}}$ most enriched in samples that are most depleted in O_2 based on the $\delta\text{O}_2/\text{Ar}$ value (Fig. 5).
302 GRIP silty ice is characterized by unusually large consumption of O_2 and very enriched $\delta^{18}\text{O}_{\text{atm}}$
303 values. These observations are all consistent with CO_2 and CH_4 concentrations, and O_2 $\delta^{18}\text{O}$
304 values observed by Souchez et al. (1995b; 2006). The most parsimonious explanation for these
305 observations is that basal ice at GRIP and Dye-3 is composed primarily of dry densified clean ice,
306 with some contribution of silty, wet origin ice. A quantification of mixing components is not
307 attempted here, but has been described in other studies (Souchez et al., 1995a; Souchez et al.,
308 1998; Verbeke et al., 2002; Bender et al., 2010).

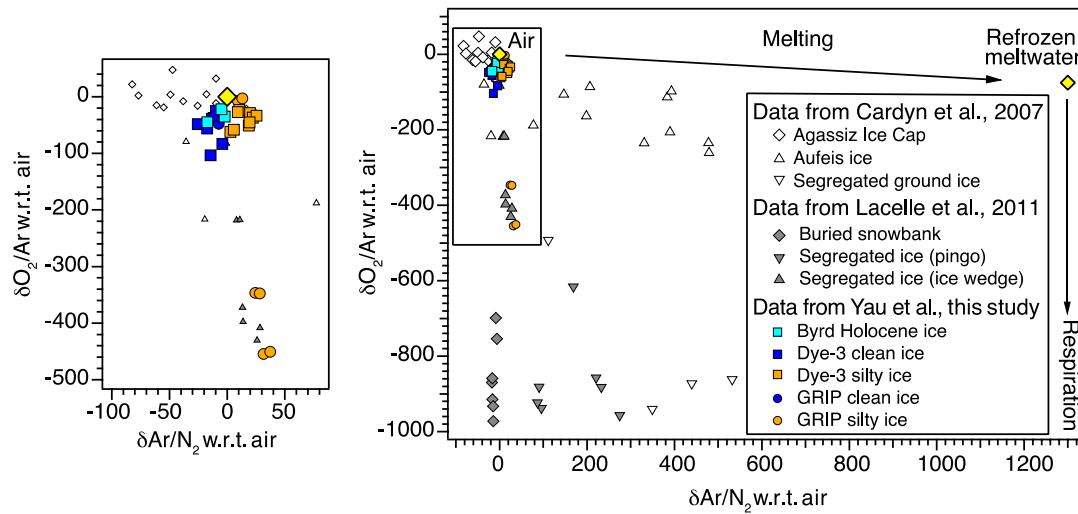
309

310 **3.3 Age Constraints on the Basal Ice of GRIP and Dye-3**

311 Dating of the trapped air reflects the average age of the dry densified glacial ice and
312 locally formed ice, with the components weighted according to their abundance and total gas
313 content. Based on the relatively high total gas content, the local ice component is likely to play a
314 small role in the Ar isotope ages of the most important samples in this study (GRIP at 3022 m
315 and Dye-3 at 2011 m depth). Table 1 summarizes the measured Ar-isotope ages for the deepest
316 ice at GRIP and Dye-3. For GRIP, 4 samples from 3020-3026 m were analyzed. The deepest

317 sample replicated poorly, with one replicate dating to the present. The anomalously young age of
318 this replicate may reflect incorporation of radiogenic ^{40}Ar from outgassing of the local
319 underlying crust, as seen in basal silty ice at GISP2 (Bender et al., 2010). Consequently, we
320 exclude this sample from our discussion of the age of the GRIP basal ice, and infer that the Ar-
321 ages from the basal ice section are lower limits because the trapped air may be contaminated
322 with crustal radiogenic ^{40}Ar . It is possible that wet origin ice could cause Ar isotope ages to be
323 older than the age of the dry densified ice. This influence would only be important if the age of
324 the trapped air from the wet origin ice was not reset by contamination associated with
325 contraction cracks (St. Jean et al., 2011), before it was overridden by dry densified glacial ice.
326 The clean GRIP sample from 3020 m depth dates to 550 ± 170 ka (n=2; 1 st. error), and the
327 remaining silty samples from 3022 m and 3025 m date to 970 ± 140 ka (n=3; 1 st. error). The
328 ^{40}Ar ages for the silty basal ice agree with the $^{10}\text{Be}/^{36}\text{Cl}$ age of Willerslev et al. (2007), 950 ± 44
329 ka. We therefore conclude that the silty basal ice from GRIP certainly dates to well before MIS
330 11 (430 ka). It is possible that the GRIP silty basal ice dates to the original build-up of the GIS,
331 as originally proposed by Souchez et al. (1994).
332

333



334

335 Fig. 4. Right: $\delta\text{Ar}/\text{N}_2$ vs. $\delta\text{O}_2/\text{Ar}$ for deep GRIP and Dye-3 ice compared with Holocene ice from
336 Byrd, Antarctica and Agassiz Ice Cap, Canada, and various deposits of wet origin ice. Left:

337 Zoom-in on GRIP and Dye-3 ice. The deepest Dye-3 and GRIP ice have $\delta\text{Ar}/\text{N}_2$ values similar to
338 that of typical dry densified ice. Some small enrichments in $\delta\text{Ar}/\text{N}_2$ may be due to regelation of

339 ice or some small mixing with a wet origin ice component. $\delta\text{O}_2/\text{N}_2$ of the silty GRIP ice indicate
340 significant respiration.

341

Table 2. Gas composition w.r.t. modern air. Each line represents a single analysis.

GRIP ice core						
Depth (m)	$\delta\text{O}_2/\text{N}_2$ (‰)	$\delta\text{O}_2/\text{Ar}$ (‰)	$\delta\text{Ar}/\text{N}_2$ (‰)	$\delta^{15}\text{N}$ (‰)	$\delta^{18}\text{O}_{\text{atm}}$ (‰)	$\delta^{18}\text{O}_{\text{ice}}$ (‰)
3020	-54.65	-47.79	-7.38	0.34	0.87	-
3020	-43.85	-33.88	-10.51	0.37	0.69	-
3022	2.18	-7.37	9.42	0.27	0.38	-34.4
3022	10.36	-2.88	13.08	0.33	0.34	-34.4
3025	-330.55	-346.50	24.30	0.46	4.87	-28.3
3025	-328.92	-347.53	28.35	0.46	4.79	-28.3
3026	-437.32	-454.58	31.51	0.50	5.91	-28.0
3026	-430.15	-450.77	37.32	0.53	5.76	-28.0

*Shaded section denotes samples from the silty basal ice

Dye-3 ice core						
Depth (m)	$\delta\text{O}_2/\text{N}_2$ (‰)	$\delta\text{O}_2/\text{Ar}$ (‰)	$\delta\text{Ar}/\text{N}_2$ (‰)	$\delta^{15}\text{N}$ (‰)	$\delta^{18}\text{O}_{\text{atm}}$ (‰)	$\delta^{18}\text{O}_{\text{ice}}$ (‰)
1991	-48.75	-37.45	-11.92	0.28	0.36	-31.1
1991	-72.38	-56.12	-17.40	0.29	0.54	-31.1
1999	-116.25	-103.53	-14.38	0.35	1.50	-31.2
1999	-87.25	-83.50	-4.29	0.25	1.25	-31.2
2004	-34.52	-25.04	-9.90	0.27	0.60	-31.0
2004	-72.29	-48.20	-25.49	0.33	0.75	-31.0
2008	-47.31	-37.29	-10.40	0.33	0.51	-31.1
2008	-51.60	-39.06	-13.23	0.30	0.65	-31.1
2011	-	-	-	-	-	-30.6
2011	-	-	-	-	-	-30.6
2014	-11.95	-31.74	20.23	0.16	0.74	-27.9
2014	-9.21	-28.54	19.71	0.17	0.68	-27.9
2015	-	-	-	-	-	-26.6
2015	-	-	-	-	-	-26.6
2019	-	-	-	-	-	-24.0
2019	-	-	-	-	-	-24.0
2023	-13.04	-23.20	10.40	0.20	0.62	-24.5
2023	-17.96	-27.12	9.22	0.13	0.70	-24.5
2027	-15.41	-36.97	22.20	0.10	0.84	-23.4
2027	-8.57	-33.40	25.50	0.07	0.81	-23.4
2031	-32.96	-50.81	18.80	0.16	0.71	-22.9
2031	-26.43	-45.15	19.43	0.07	0.91	-22.9
2035	-59.20	-62.08	2.88	0.11	1.10	-22.8
2035	-52.69	-58.27	5.74	0.12	1.01	-22.8

*Shaded section denotes samples from the silty basal ice

Table 3. Total Air Content

GRIP ice core		Dye-3 ice core	
Depth (m)	Air Content (scc/g)	Depth (m)	Air Content (scc/g)
3022.3	0.098	2010.9	0.081
3022.5	0.084	2012.5	0.089
3022.6	0.068	2014.1	0.069
3022.9	0.077	2014.5	0.089
3023.3	0.087	2015.3	0.090
3023.7	0.077	2016.1	0.053
3024.1	0.080	2016.7	0.067
3024.4	0.068	2018.3	0.061
3024.7	0.070	2021.7	0.068
3025.1	0.063	2022.7	0.060
3025.5	0.058	2023.3	0.075
3025.7	0.074	2024.7	0.053
3026.2	0.065	2025.3	0.065
3026.4	0.068	2027.1	0.056
3026.6	0.072	2027.5	0.057
3027.3	0.059	2028.7	0.064
3027.9	0.051	2029.1	0.053
3028.3	0.048	2029.7	0.053
3028.6	0.048	2031.1	0.052
		2032.1	0.055
		2032.9	0.059
		2033.9	0.047
		2034.7	0.059
		2035.5	0.059
		2035.9	0.052
		2036.7	0.062
		2037.4	0.051
		2037.8	0.036

*Data for GRIP from Souchez et al. (1995a). Data for Dye-3 from Souchez et al. (1998). For Dye-3, Units 1-3, as defined by Souchez et al. (1998), are noted by shading.

344

345

For Dye-3, 1 sample was analyzed from the clean section, and 4 from the silty section;

346

one sample was replicated from each section. The average age for the silty basal ice is 210 ± 110

347

kyr (1 st. error, n=2) in the future. This means that there is excess ^{40}Ar in the basal ice at Dye-3

348

that is driving the $\delta^{40}\text{Ar}/^{38}\text{Ar}_{\text{atm}}$ value above that of the modern atmosphere. The amount of

349

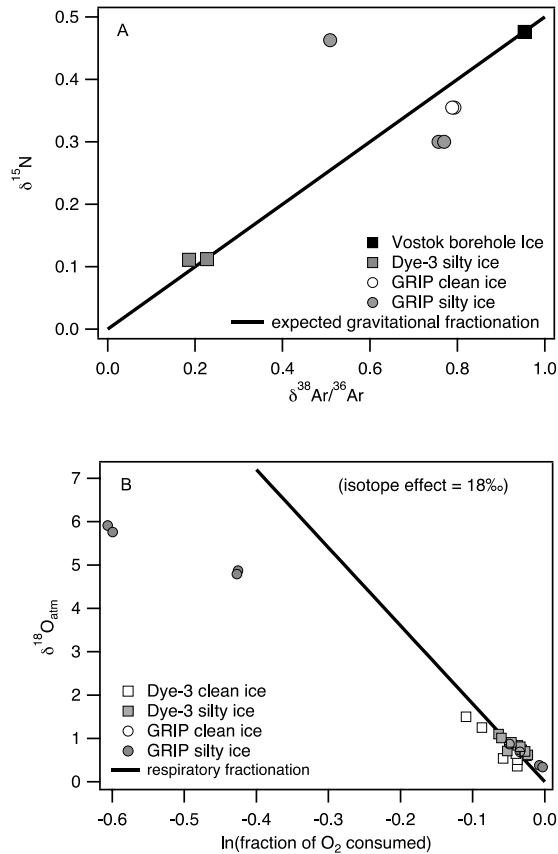
excess ^{40}Ar far exceeds the amount that could be generated from radiogenic ^{40}Ar produced by

350 just the silt and debris in the ice (weight % between 0.05-0.6%, Olmez et al., 1993). The likely
351 source of excess ^{40}Ar is outgassing of radiogenic ^{40}Ar from the underlying continental crust, as is
352 seen at GISP2 and GRIP (Bender et al., 2010; this work).

353 The Ar-isotope age for replicates from the clean ice (2011 m) is 400 ± 170 ka (1 st. error,
354 $n=2$). This result is fully consistent with data in Willerslev et al. (2007) suggesting an age of 400-
355 800 ka for basal ice at Dye-3. However, the large Ar age uncertainty prevents a definitive
356 conclusion at the 95% confidence level that Dye-3 was ice-covered during the Eemian.
357 Consequently, analyses of $^{17}\Delta$ of O_2 are performed to further constrain the age.

358 For at least the past 400 ka, $^{17}\Delta$ has varied systematically with climate and atmospheric
359 CO_2 (Fig. 3). Interglacial $^{17}\Delta$ typically averages -5 to +10 per meg, while glacial values average
360 between +35 and +45 per meg (Blunier et al., 2002; Blunier et al., 2012). With an analytical
361 uncertainty of ± 6 per meg, $^{17}\Delta$ can date trapped air to glacial or interglacial times.

362 Following Oeschger et al. (1983), we believe that Dye-3 is basically stratigraphically
363 intact back to about 60 ka (Fig. 2). In this view, the $\delta^{18}\text{O}$ peak at 1932 m corresponds to
364 Interstadial 12 in GISP2 and GRIP (~48 ka). The maximum at 1935 m corresponds to
365 Interstadial 13, and the maximum at 1945 m corresponds to Interstadial 14. At 1956 m and 1958
366 m in Dye-3, 2 isotope maxima correspond to Interstadial 15 and the short unnumbered
367 interstadial that follows. Then at 1955 m and 1958 m depth, two particularly warm events
368 separated by a cold event correspond to Interstadials 16 and 17 in GISP2 and GRIP. According
369 to these correlations, Dye-3 has an age of 60 ka at 1959 m depth, and deeper ice is presumed to
370 be older.



371
 372 Fig. 5. A. Plot of $\delta^{38}\text{Ar}/^{36}\text{Ar}$ vs. $\delta^{15}\text{N}$. The heavy black line is the expected mass-dependent
 373 gravitational fractionation. A Vostok borehole (~100 m depth) sample illustrates how air from
 374 typical ice is fractionated. The Dye-3 silty ice and GRIP clean ice are gravitationally fractionated,
 375 though we observe scatter in the deepest silty GRIP samples. B. Plot of the fraction of O_2
 376 consumed (based on the deviation of O_2/Ar from the atmospheric ratio) vs. $\delta^{18}\text{O}_{\text{atm}}$. The heavy
 377 black line is the Rayleigh fractionation relationship assuming a respiratory isotope effect of 18‰.
 378 Samples from the deep Dye-3 (clean and silty) and GRIP (clean) ice plot along this line,
 379 indicating that some O_2 in the trapped air has been consumed by respiration. GRIP silty basal ice
 380 samples show an unusually large degree of consumption. Our $\delta^{18}\text{O}$ data are similar to earlier
 381 results of Souchez et al. (2006).
 382

383 With this constraint, we use $^{17}\Delta$ to determine the youngest probable age of the trapped air.
384 Fig. 3 shows the results of the $^{17}\Delta$ analyses. 4 clean ice samples had $^{17}\Delta$ values of $+42 \pm 9$ per
385 meg (1 σ ; st. error = ± 4 per meg). 4 samples of silty ice had $^{17}\Delta$ values of $+45 \pm 7$ per meg (1 σ ; st.
386 error = ± 4 per meg). These are diagnostic of glacial maximum air and (inferentially) ice (Fig. 3).
387 Given that the minimum age for the deep ice is 60 ka, and that prior to this time, $^{17}\Delta$ values of
388 ~ 43 per meg were not realized until ~ 132 ka, we conclude that Dye-3 was ice-covered through
389 the LIG. This interglacial was exceptionally warm. It thus seems likely that the GIS at Dye-3 was
390 intact since the unusually long Marine Isotope Stage 11, and perhaps at earlier times.

391

392 **4. Conclusions**

393 We have analyzed the concentration and isotopic composition of O₂, N₂ and Ar in
394 trapped gases from clean and silty basal ice from the GISP2 and DYE-3 ice cores. Ar/N₂ ratios,
395 and $\delta^{15}\text{N}$ of N₂, confirm earlier work (including Souchez et al., 2006) suggesting that trapped
396 gases in silty ice derive primarily from clean, dry densified ice in most samples. $^{40}\text{Ar}/^{38}\text{Ar}$ ratios
397 constrain ages with an uncertainty of 150-250 ka for a single sample. Contamination by crustal
398 radiogenic ^{40}Ar make ice ages minimum ages, and in Dye-3 the deepest samples have ages in the
399 future. These limitations notwithstanding, our data have significant implications for the history
400 of the Greenland Ice Sheet.

401 Analyses of the trapped air from the GRIP and Dye-3 basal ice indicate a relatively
402 resilient GIS. Ar-isotope dating of air from the silty basal ice gives a minimum age for the ice
403 sheet at Summit of 970 ± 140 ka (1 st. error), suggesting that the GIS at Summit survived
404 through MIS 11 despite significant collapse of the GIS (Raymo and Mitrovica, 2012). In addition,
405 evidence that the ice sheet at Dye-3 survived the last interglacial comes from two Ar-isotope

406 dates averaging 400 ± 170 ka (1 st. error). $^{17}\Delta$ stratigraphy further constrains the minimum age to
407 ~ 132 ka. Ice dating to the last interglacial was not found in the depth interval studied (1991-2035
408 m), and does not appear to be present at shallower depths, where $\delta^{18}\text{O}_{\text{ice}}$ values do not reach
409 Holocene values ($\sim -28\%$; Johnsen et al., 2001). We presume that ice dynamics removed Eemian
410 ice from the Dye-3 site, but the record holds no information about how this might have happened.

411 It remains a matter of investigation whether the ice sheet at Dye-3 was a part of the main
412 body of the GIS, or whether an ice dome at Southern Greenland was present during the Eemian
413 (Cuffey and Marshall, 2000; Huybrechts, 2002; Tarasov and Peltier, 2003; Lhomme et al., 2005).
414 Our results do not preclude extensive melting of the ice sheet over the LIG, as changes at the
415 margin as well as in coastal northern Greenland could have been extensive (Born and
416 Nisancioglu, 2012), and the net elevation change at Dye-3 during the LIG is unknown.

417 Our data indicate that the GIS did not completely melt at Southern Greenland during the
418 Eemian, nor did it completely melt at Summit Greenland during MIS 11. These constraints on
419 the trapped air of basal ice from GRIP and Dye-3 are in line with estimates of the age and
420 stability of the GIS from Willerslev et al. (2007), Colville et al. (2011), and Reyes et al. (2014).

421

422

423 **Acknowledgements**

424 This work was supported by the National Science Foundation, Polar Programs, under Grant
425 0636731, and the BP Amoco – Princeton University Carbon Mitigation Initiative. We are deeply
426 indebted to Jean-Louis Tison and an anonymous reviewer whose comments significantly
427 improved the manuscript.

428

429

430 **References**

- 431
- 432 Bamber, J.L., Griggs, J.A., Hurkmans, R., Dowdeswell, J.A., Gogineni, S.P., Howat, I.,
- 433 Mouginit, J., Paden, J., Palmer, S., Rignot, E., Steinhage, D., 2013. A new bed elevation
- 434 dataset for Greenland. *Cryosphere* 7, 499-510.
- 435 Bender, M., Sowers, T., Lipenkov, V., 1995. On the concentrations of O-2, N-2, and Ar in
- 436 trapped gases from ice cores. *J. Geophys. Res.-Atmos.* 100, 18651-18660.
- 437 Bender, M.L., Barnett, B., Dreyfus, G., Jouzel, J., Porcelli, D., 2008. The contemporary
- 438 degassing rate of Ar-40 from the solid Earth. *Proceedings of the National Academy of*
- 439 *Sciences of the United States of America* 105, 8232-8237.
- 440 Bender, M.L., Burgess, E., Alley, R.B., Barnett, B., Clow, G.D., 2010. On the nature of the dirty
- 441 ice at the bottom of the GISP2 ice core. *Earth Planet. Sci. Lett.* 299, 466-473.
- 442 Blunier, T., Barnett, B., Bender, M.L., Hendricks, M.B., 2002. Biological oxygen productivity
- 443 during the last 60,000 years from triple oxygen isotope measurements. *Glob. Biogeochem.*
- 444 *Cycle* 16, DOI: 10.1029/2001gb001460.
- 445 Blunier, T., Bender, M.L., Barnett, B., von Fischer, J.C., 2012. Planetary fertility during the past
- 446 400 ka based on the triple isotope composition of O-2 in trapped gases from the Vostok
- 447 ice core. *Clim. Past.* 8, 1509-1526.
- 448 Boereboom, T., Samyn, D., Meyer, H., and Tison, J. L., 2013. Stable isotope and gas properties
- 449 of two climatically contrasting (Pleistocene and Holocene) ice wedges from Cape
- 450 Mamontove Klyk, Laptev Sea, northern Siberia. *Cryosphere* 7, 31-46.
- 451 Born, A., Nisancioglu, K.H., 2012. Melting of Northern Greenland during the last interglaciation.
- 452 *Cryosphere* 6, 1239-1250.
- 453 Cardyn, R., Clark, I.D., Lacelle, D., Lauriol, B., Zdanowicz, C., Calmels, F., 2007. Molar gas

454 ratios of air entrapped in ice: A new tool to determine the origin of relict massive ground
455 ice bodies in permafrost. *Quat. Res.* 68, 239-248.

456 Chapman, S., Cowling, T.G., 1970. *The Mathematical Theory of Non-Uniform Gases.*
457 Cambridge University Press.

458 Chappellaz, J., Brook, E., Blunier, T., Malaize, B., 1997. CH₄ and δ¹⁸O of O₂ records from
459 Antarctic and Greenland ice: a clue for stratigraphic disturbance in the bottom part of the
460 Greenland Ice Core Project and the Greenland Ice Sheet Project 2 ice cores. *J. Geophys.*
461 *Res.* 102, 26547–26557.

462 Clark, P.U., Huybers, P., 2009. GLOBAL CHANGE Interglacial and future sea level. *Nature* 462,
463 856-857.

464 Colville, E.J., Carlson, A.E., Beard, B.L., Hatfield, R.G., Stoner, J.S., Reyes, A.V., Ullman, D.J.,
465 2011. Sr-Nd-Pb Isotope Evidence for Ice-Sheet Presence on Southern Greenland During
466 the Last Interglacial. *Science* 333, 620-623.

467 Craig, H., Horibe, Y., Sowers, T., 1988. Gravitational separation of gases and isotopes in polar
468 ice caps. *Science* 242, 1675-1678.

469 Cuffey, K.M., Marshall, S.J., 2000. Substantial contribution to sea-level rise during the last
470 interglacial from the Greenland ice sheet. *Nature* 404, 591-594.

471 Dahl-Jensen, D., Community, NEEM., 2013. Eemian interglacial reconstructed from a
472 Greenland folded ice core. *Nature* 493, 489-494.

473 Dreyfus, G.B., Parrenin, F., Lemieux-Dudon, B., Durand, G., Masson-Delmotte, V., Jouzel, J.,
474 Barnola, J.M., Panno, L., Spahni, R., Tisserand, A., Siegenthaler, U., Leuenberger, M.,
475 2007. Anomalous flow below 2700 m in the EPICA Dome C ice core detected using delta
476 O-18 of atmospheric oxygen measurements. *Clim. Past.* 3, 341-353.

477 Emerson, S., Quay, P.D., Stump, C., Wilbur, D., Schudlich, R., 1995. Chemical tracers of
478 productivity and respiration in the subtropical Pacific Ocean. *J. Geophys. Res.-Oceans*
479 100, 15873-15887.

480 Herron, M.M., Langway, C.C., 1980. Firn densification – an empirical model. *J. Glaciol.* 25,
481 373-385.

482 Herron, M.M., Langway, C.C., 1987. Derivation of paleoelevations from total air content of two
483 deep Greenland ice cores. *The Physical Basis of Ice Sheet Modelling, Proceedings of the*
484 *Vancouver Symposium. IAHS 170.*

485 Huybrechts, P., 2002. Sea-level changes at the LGM from ice-dynamic reconstructions of the
486 Greenland and Antarctic ice sheets during the glacial cycles. *Quat. Sci. Rev.* 21, 203-231.

487 Johnsen, S.J., Dahl-Jensen, D., Gundestrup, N., Steffensen, J.P., Clausen, H.B., Miller, H.,
488 Masson-Delmotte, V., Sveinbjornsdottir, A.E., White, J., 2001. Oxygen isotope and
489 palaeotemperature records from six Greenland ice-core stations: Camp Century, Dye-3,
490 GRIP, GISP2, Renland and NorthGRIP. *J. Quat. Sci.* 16, 299-307.

491 Knight, P.G., 1997. The basal ice layer of glaciers and ice sheets. *Quat. Sci. Rev.* 16, 975-993.

492 Koerner, R.M., 1989. Ice core evidence for extensive melting of the Greenland ice-sheet in the
493 last interglacial. *Science* 244, 964-968.

494 Koerner, R.M., Fisher, D.A., 2002. Ice-core evidence for widespread Arctic glacier retreat in the
495 Last Interglacial and the early Holocene, in: Wolff, E.W. (Ed.), *Ann. Glaciol* 35, 19-24.

496 Kopp, R.E., Simons, F.J., Mitrovica, J.X., Maloof, A.C., Oppenheimer, M., 2009. Probabilistic
497 assessment of sea level during the last interglacial stage. *Nature* 462, 863-867.

498 Lacelle, D., Radtke, K., Clark, I.D., Fisher, D., Lauriol, B., Utting, N., Whyte, L.G., 2011.
499 Geomicrobiology and occluded O-2-CO2-Ar gas analyses provide evidence of microbial

500 respiration in ancient terrestrial ground ice. *Earth Planet. Sci. Lett.* 306, 46-54.

501 Lhomme, N., Clarke, G.K.C., Marshall, S.J., 2005. Tracer transport in the Greenland Ice Sheet:
502 constraints on ice cores and glacial history. *Quat. Sci. Rev.* 24, 173-194.

503 Luz, B., Barkan, E., Bender, M.L., Thiemens, M.H., Boering, K.A., 1999. Triple-isotope
504 composition of atmospheric oxygen as a tracer of biosphere productivity. *Nature* 400,
505 547-550.

506 Martinerie, P., Raynaud, D., Etheridge, D.M., Barnola, J.M., Mazaudier, D., 1992. Physical and
507 climatic parameters which influence the air content in polar ice. *Earth Planet. Sci. Lett.*
508 112, 1-13.

509 Oeschger, H., Beer, J., Siegenthaler, U., Stauffer, B., Dansgaard, W., Langway, C.C., 1983. Late
510 Glacial Climate History from Ice Cores. *Paleoclimate Research Models*. DOI:
511 10.1007/978-94-009-7236-0_12

512 Olmez, I., Fireman, E.L., Langway, C.C., 1993. Trace-elements in basal ice at Dye-3.
513 *Atmospheric Environment Part A-General Topics* 27, 2921-2926.

514 Raymo, M.E., Mitrovica, J.X., 2012. Collapse of polar ice sheets during the stage 11 interglacial.
515 *Nature* 483, 453-456.

516 Reyes, A.V., Carlson, A.E., Beard, B.L., Hatfield, R.G., Stoner, J.S., Winsor, K., Welke, B.,
517 Ullman, D.J., 2014. South Greenland ice-sheet collapse during Marine Isotope Stage 11.
518 *Nature* 510, 525-528.

519 Schwander, J., 1989. The transformation of snow to ice and the occlusion of gases, in: Oeschger,
520 H., Langway, C. (Eds.), *The Environmental Record in Glaciers and Ice Sheets*. John Wiley,
521 New York.

522

523 St. Jean, M., Lauriol, B., Clark, I. D., Lacelle, D., and Zdanowicz, C., 2011. Investigation of ice-
524 wedge infilling processes using stable oxygen and hydrogen isotopes, crystallography
525 and occluded gases (O₂, N₂, Ar). *Permafrost and Periglac. Process.* 22, 49-64.

526 Severinghaus, J.P., Grachev, A., Battle, M., 2001. Thermal fractionation of air in polar firn by
527 seasonal temperature gradients. *Geochem. Geophys. Geosyst.* 2, 2000GC000146.

528 Severinghaus, J.P., Albert, M.R., Courville, Z.R., Fahnestock, M.A., Kawamura, K., Montzka,
529 S.A., Muhle, J., Scambos, T.A., Shields, E., Shuman, C.A., Suwa, M., Tans, P., Weiss,
530 R.F., 2010. Deep air convection in the firn at a zero-accumulation site, central Antarctica.
531 *Earth Planet. Sci. Lett.* 293, 359-367.

532 Souchez, R., Lorrain, R., Tison, J.L., Jouzel, J., 1988. Co-isotopic signature of two mechanisms
533 of basal-ice formation in arctic outlet glaciers. *Ann. Glaciol* 10, 163-166.

534 Souchez, R., Tison, J.L., Lorrain, R., Lemmens, M., Janssens, L., Stievenard, M., Jouzel, J.,
535 Sveinbjornsdouir, A., Johnsen, S.J., 1994. Stable isotopes in the basal silty ice preserved
536 in the Greenland Ice Sheet at Summit; environmental implications. *Geophys. Res. Lett.*
537 21, 693-696.

538 Souchez R., Janssens, L., Lemmens, M., 1995a. Very low oxygen concentration in basal ice from
539 Summit, Central Greenland, *Geophys. Res. Lett.* 22, 2001-2004.

540 Souchez, R., Lemmens, M., Chappellaz, J., 1995b. Flow-induced mixing in the GRIP basal ice
541 deduced from the CO₂ and CH₄ records, *Geophys. Res. Lett.* 22, 41-44.

542 Souchez, R., 1997. The buildup of the ice sheet in central Greenland. *J. Geophys. Res.-Oceans*
543 102, 26317-26323.

544 Souchez, R., Bouzette, A., Clausen, H.B., Jonsen, S.J., Jouzel, J., 1998. A stacked mixing
545 sequence at the base of the Dye-3 core, Greenland. *Geophys. Res. Lett.* 25, 1943-1946.

546 Souchez, R., Jouzel, J., Landais, A., Chappellaz, J., Lorrain, R., Tison, J.L., 2006. Gas isotopes
547 in ice reveal a vegetated central Greenland during ice sheet invasion. *Geophys. Res. Lett.*
548 33, L24503.

549 Sowers, T., Bender, M., Raynaud, D., 1989. Elemental and isotopic composition of occluded O-2
550 and N-2 in polar ice. *J. Geophys. Res.-Atmos.* 94, 5137-5150.

551 Suwa, M., von Fischer, J.C., Bender, M.L., Landais, A., Brook, E.J., 2006. Chronology
552 reconstruction for the disturbed bottom section of the GISP2 and the GRIP ice cores:
553 Implications for Termination II in Greenland. *J. Geophys. Res.-Atmos.* 111, DOI:
554 10.1029/2005JD006032.

555 Tarasov, L., Peltier, W.R., 2003. Greenland glacial history, borehole constraints, and Eemian
556 extent. *J. Geophys. Res.-Solid Earth* 108, DOI: 10.1029/2001JB001731.

557 Tison, J.-L., Thorsteinsson, T., Lorrain, R.D., Kipfstuhl, J., 1994. Origin and development of
558 textures and fabrics in basal ice at Summit, Central Greenland. *Earth and Planetary
559 Science Letters* 125, 421-437.

560 Tison, J.-L., Souchez, R., Wolff, E. W., Moore, J. C., Legrand, M. R., de Angelis, M., 1998. Is a
561 periglacial biota responsible for enhanced dielectric response in basal ice from the
562 Greenland Ice Core Project ice core? *J. Geophys. Res.* 103, 18,885-18,894.

563 Verbeke, V., Lorrain, R., Johnsen, S.J., Tison, J., 2002. A multiple-step deformation history of
564 basal ice from the Dye 3 (Greenland) core: new insights from the CO₂ and CH₄ content.
565 *Annals of Glaciology* 35, 231-236.

566 Willerslev, E., Cappellini, E., Boomsma, W., Nielsen, R., Hebsgaard, M.B., Brand, T.B.,
567 Hofreiter, M., Bunce, M., Poinar, H.N., Dahl-Jensen, D., Johnsen, S., Steffensen, J.P.,
568 Bennike, O., Schwenninger, J.L., Nathan, R., Armitage, S., de Hoog, C.J., Alfimov, V.,

569 Christl, M., Beer, J., Muscheler, R., Barker, J., Sharp, M., Penkman, K.E.H., Haile, J.,
570 Taberlet, P., Gilbert, M.T.P., Casoli, A., Campani, E., Collins, M.J., 2007. Ancient
571 biomolecules from deep ice cores reveal a forested Southern Greenland. *Science* 317,
572 111-114.

573 Yau, A.M., 2014. Extending polar ice core records: Studies on the trapped air of glacial ice from
574 Antarctica, Greenland, and the Canadian Arctic. Princeton University, PhD Thesis
575 Dissertation.

576

577